Supporting Information for

Network Cracks-based Wearable Strain Sensors for both Subtle and Large Strain Detection of Human Motions

Shuai Wang,[a] Peng Xiao,[a] Yun Liang,[a] Jiawei Zhang,[a] Youju Huang,*[a, b] Si Wu,[b] Shiao-Wei Kuo,[c] and Tao Chen*[a]

[a]*Ningbo Institute of Material Technology and Engineering, Key Laboratory of Graphene Technologies and Applications of Zhejiang Province, Chinese Academy of Sciences, Ningbo, 315201, China. University of Chinese Academy of Sciences, 19A Yuquan Road, Beijing 100049, China. E-mail: tao.chen@nimte.ac.cn*

[b]*Max Planck Institute for Polymer Research, Ackermannweg 10, D-55128, Mainz, German. Email: huangyouju@mpip-mainz.mpg.de*

[c]*Department of Material and Optoelectronic Science, National Sun Yat-Sen University, 804, Kaohsiung, Taiwan*

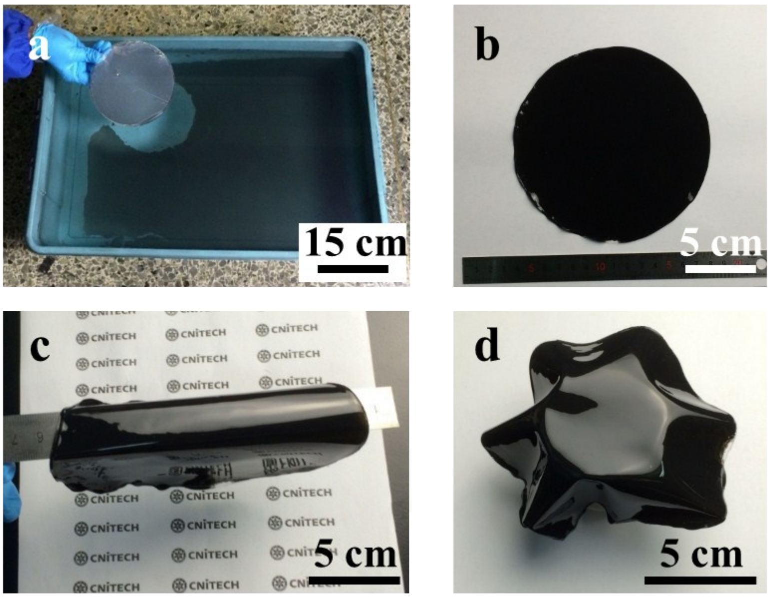

Figure S1. a) Optical image showing the CNT film transferred by a circle substrate. b) Multilayer CNTs films/PDMS composite after PDMS curing. The flexible CNTs films/PDMS composite film put on c) a steel ruler, d) a beaker.

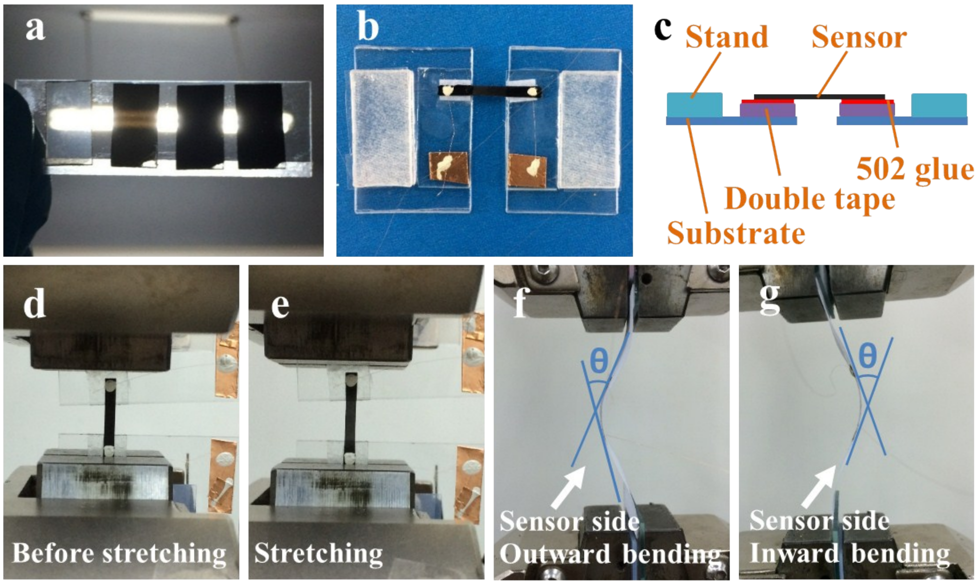

Figure S2. a) Transmittance of different layers of CNTs films. b) Optical image of the home-made device. c) Illustration of the cross view of the fixing device in b. d-e) The stretching and releasing test using Instron 5567. f-g) The outward bending and inward bending test of the strain sensor fixed on a paper substrate.

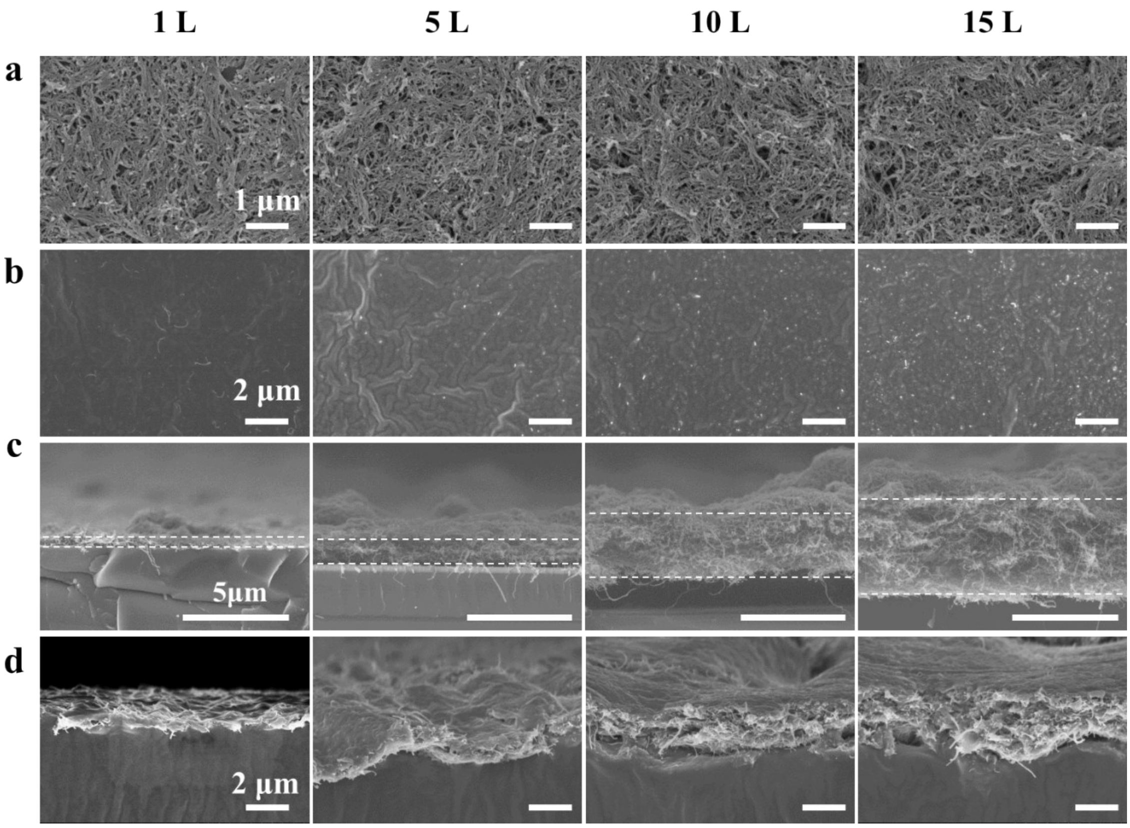

Figure S3. a) Top view SEM images of the CNTs films. b) Top view SEM images of the CNTs films/PDMS composite. c) Cross-sectional SEM images of the CNTs films. d) Cross-sectional SEM images of the CNTs films/PDMS composite.

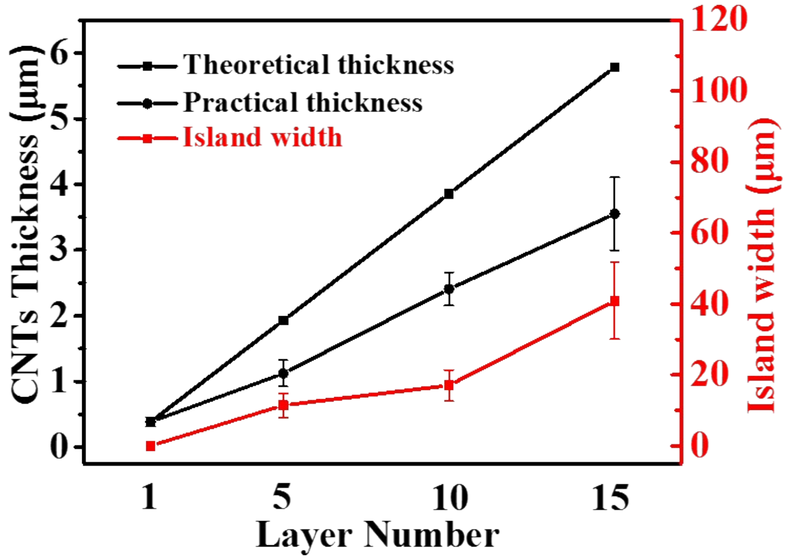

Figure S4. a) Theoretical thickness (top black line), practical thickness (middle black line) of CNTs films and island width (bottom red line) of CNTs films/PDMS strain sensors versus layer number.

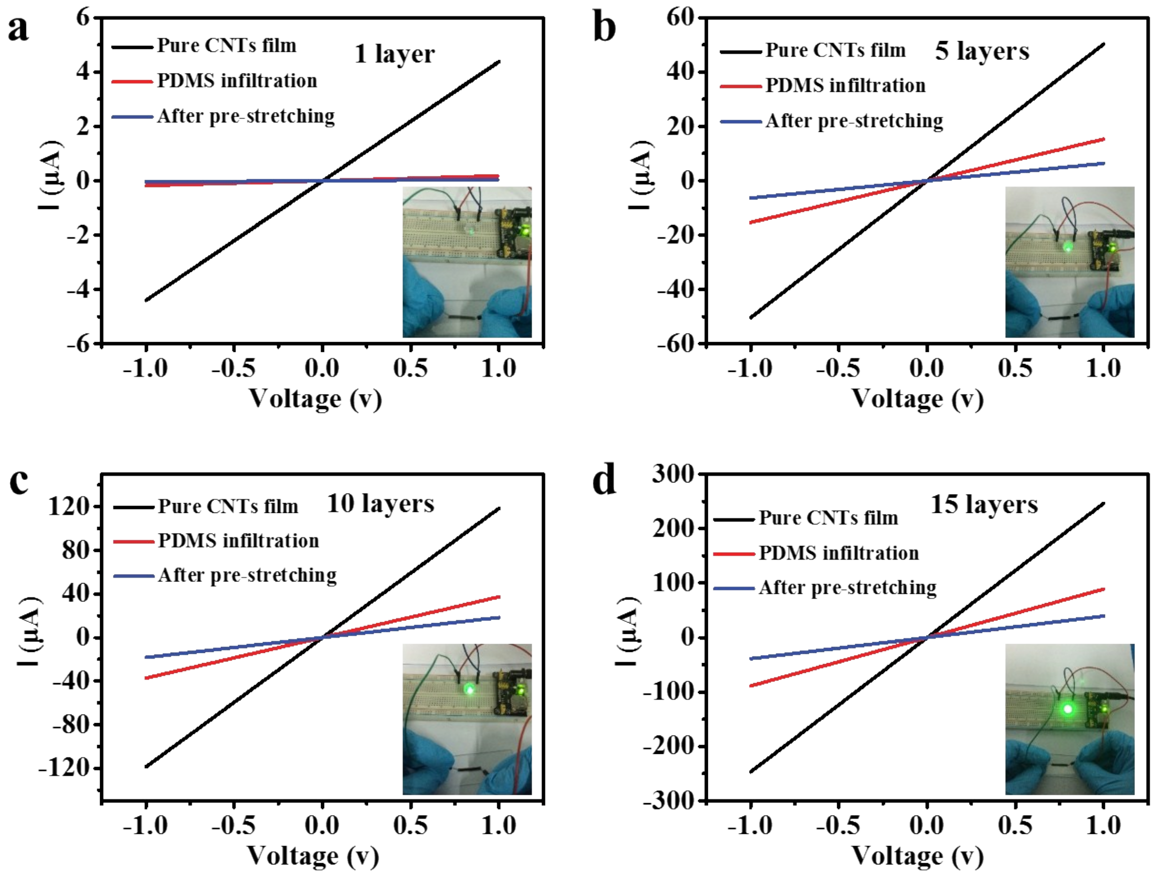

Figure S5. Current-voltage curves of CNTs film, CNTs films/PDMS composite, CNTs films/PDMS composite after pre-stretching. Insets: optical images showing the light intensity of a green LED (CNTs films/PDMS composite before pre-stretching).

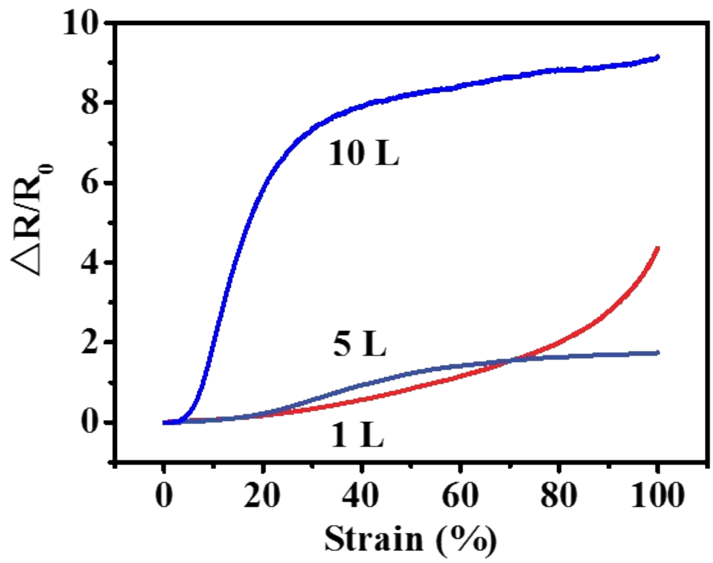

Figure S6. The relative change in resistance versus strain curves of 1, 5, 10layers of CNTs films/PDMS strain sensors, showing varied GF behaviors.

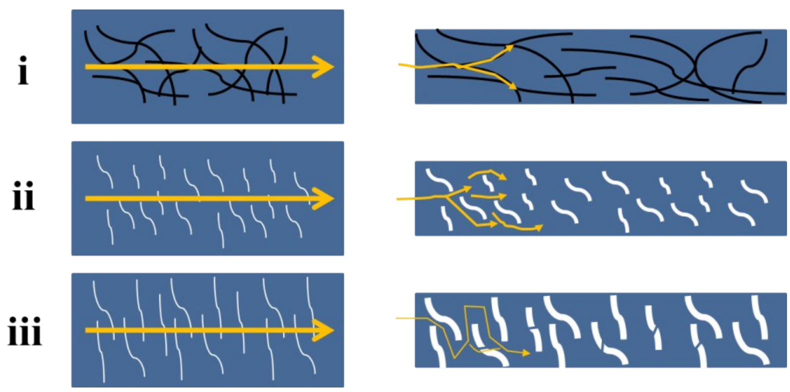

Figure S7. Schematic showing current flow pathways through embedded CNTs percolation (i for 1 layer) and network cracks (ii for 5 layers and iii for 10, 15 layers) with strain loading.

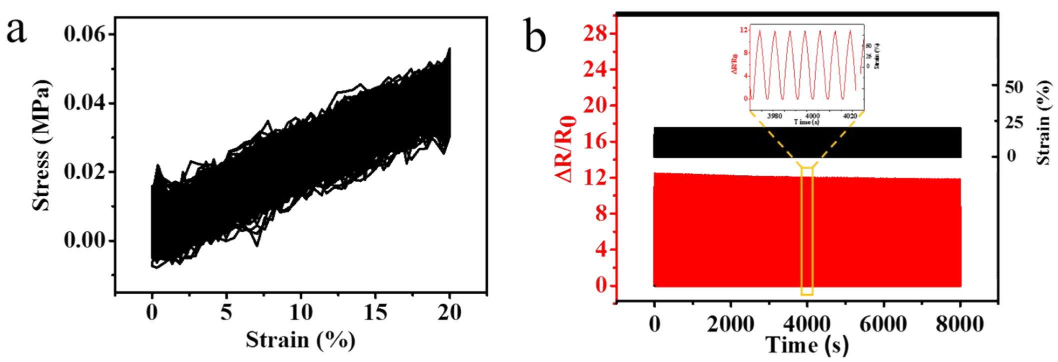

Figure S8. a) Mechanical durability test and b) its corresponding change in resistance of the 15 layers of CNTs films/PDMS strain sensor with repeated cycles (1000 cycles) of stretching and releasing of 20% strain.

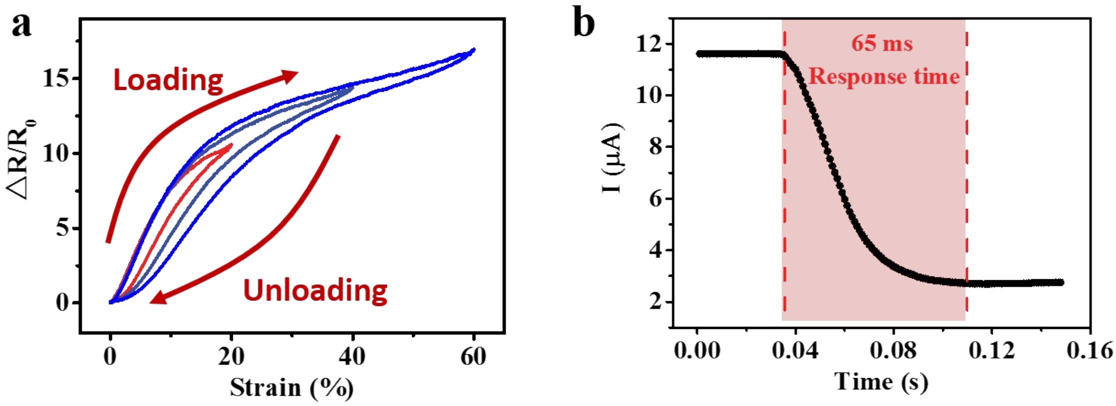

Figure S9. a) Hysteresis curve under 20, 40, 60% and b) response time curve of the 15 layers of CNTs films/PDMS strain sensor.

Table S1 Comparison with other reported crack based strain sensors.

Materials	Max strain	Gauge factor	Durability	Pulse detection with P, T, D signal	Finger bending sensing
Platinum (Pt) layer/polyurethane acrylate (PUA)[1]	2%	2000	500cycles @ 2% strain	√	×
Graphene/lightly cross-linked polysilicone[2]	10%	535	Not shown	√	√
Ag NWs@P-PDMS[3]	60%	150000	35000 cycles @ 25% strain	×	√
Fish-scale-like graphene-sensing layer/elastic adhesive tape[4]	82%	16.2-150	5000 cycles @ 10%	×	√
Aligned SWCNT/PDMS[5]	280%	0.82 (0-40%) 0.06 (>60%)	10000 cycles @ 150% strain	×	√
Self-similar wrinkles CNT-Ecoflex[6]	750%	0.65 (0-400%) 48 (400-700%)	1000 cycles @ 500%	×	√
CNTs films/PDMS (This work)	100%	87 (0-40%) 6 (>60%)	1500 cycles@20% strain	√	√

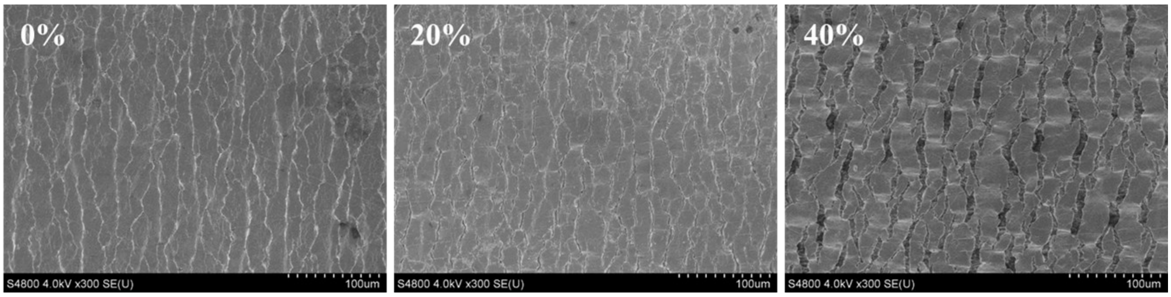

Figure S10. Mechanical deformation: top view SEM images of the CNTs films/PDMS strain sensor with network cracks under 0%, 20%, 40% strain.

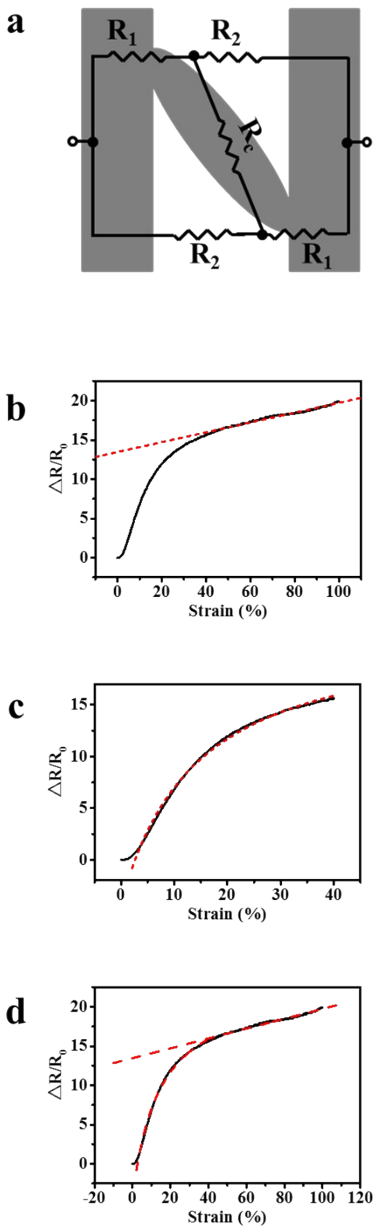

From the configuration

$$R = \frac{R_1R_C + 2R_1R_2 + R_2R_C}{R_1 + 2R_C + R_2}$$

$$R_1 = \text{const.}$$

At high strain (＞40%)

$$R_2 \gg R_1, R_c$$

$$R = \frac{R_1R_C/R_2 + 2R_1 + R_C}{R_1/R_2 + 2R_C/R_2 + 1} = 2R_1 + R_C$$

Fitted with blue line

$$R_1 = 442\ (\mathrm{K\Omega})$$

$$R_c(\mathrm{K\Omega}) = 384(\mathrm{K\Omega}) \times strain(\%)$$

Below 40% strain

$$R_1 = \text{const.}$$

$$R_c \approx \text{const.}$$

$$R_2 \sim strain.$$

$$R = \frac{R_1R_C + 2R_1R_2 + R_2R_C}{R_1 + 2R_C + R_2}$$

$$= \frac{R_1R_C + (2R_1 + R_C)R_2}{R_1 + 2R_C + R_2}$$

$$= \frac{a + bR_2}{c + R_2}$$

a, b, c are const.

Figure S11. Resistance model. a) Schematic description of the resistance model of a sensing unit the basic components. b) Determination of R_1 and R_c at high strain. c) Determination of R from R_1, R_2 and R_c. d) Overlaid plot of the model curve (red dashed line) with the experimental data (black solid line).

References

1 D. Kang, P. V. Pikhitsa, Y. W. Choi, C. Lee, S. S. Shin, L. Piao, B. Park, K.-Y. Suh, T.-i. Kim and M. Choi, *Nature*, 2014, **516**, 222.

2 C. S. Boland, U. Khan, G. Ryan, S. Barwich, R. Charifou, A. Harvey, C. Backes, Z. Li, M. S. Ferreira, M. E. Mobius, R. J. Young and J. N. Coleman, *Science*, 2016, **354**, 1257.

3 X. Liao, Z. Zhang, Z. Kang, F. Gao, Q. Liao and Y. Zhang, *Mater. Horiz.*, 2017, **4**, 502.

4 Q. Liu, J. Chen, Y. Li and G. Shi, *ACS Nano*, 2016, **10**, 7901.

5 T. Yamada, Y. Hayamizu, Y. Yamamoto, Y. Yomogida, A. Izadi-Najafabadi, D. N. Futaba and K. Hata, *Nat. Nanotechnol.*, 2011, **6**, 296.

6 S. J. Park, J. Kim, M. Chu and M. Khine, *Advanced Materials Technologies,* 2016, **1**, 1600053.